PHYSICAL REVIEW B **88**, 161108(R) (2013)

Nonempirical generalized gradient approximation free-energy functional for orbital-free simulations

Valentin V. Karasiev,* Debajit Chakraborty, Olga A. Shukruto, and S. B. Trickey
Quantum Theory Project, Departments of Physics and Chemistry, P.O. Box 118435, University of Florida, Gainesville, Florida 32611-8435, USA
(Received 6 August 2013; published 28 October 2013)

We report a purely nonempirical generalized gradient approximation for the noninteracting free energy functional of orbital-free density functional theory obtained via a novel constraint-based parametrization scheme. We use that functional to provide forces for finite-temperature molecular dynamics simulations in the warm dense matter (WDM) regime and demonstrate good-to-excellent agreement with reference Kohn-Sham calculations under WDM conditions at a minuscule fraction of the computational cost of corresponding orbital-based simulations.

DOI: 10.1103/PhysRevB.88.161108 PACS number(s): 71.15.Mb, 05.70.Ce, 31.15.E−, 65.40.G−

Compared to ordinary condensed matter, the warm dense matter (WDM) regime[1,2] poses experimental accessibility issues (e.g., inertial confinement fusion hohlraums[3]) that make computational characterization of WDM thermodynamics particularly significant. Current practice, for example Refs. 4,5, is *ab initio* molecular dynamics (AIMD) with Born-Oppenheimer electronic forces on the ions from finite-T Kohn-Sham (KS) density functional[6–8] calculations. Computational costs for KS-AIMD scale no better than N_b^3 per MD step, with N_b the number of occupied KS orbitals. N_b grows unfavorably with increasing T. KS-AIMD thus becomes prohibitively expensive at elevated T and path-integral Monte Carlo (PIMC) simulations, which have comparable computational cost, come into play.[2]

A long-standing potential alternative to KS-DFT, orbital-free DFT (OFDFT), would scale linearly with system size. Use of OFDFT for WDM has been limited by clearly inadequate functionals, e.g., Thomas-Fermi,[9] for the noninteracting kinetic energy (KE) part $\mathcal{T}_s$ of the free energy (though TF is, of course, the proper KS limit for high T and high material densities[5]). Ground-state two-point orbital-free KE functionals[10] are, unfortunately, of little utility for extension to WDM because those two-point functionals which treat different material phases equally well are both parametrized and introduce substantial extra computational complexity. Therefore we have focused on single-point functionals.

Here we present a purely constraint-based parametrization scheme for the generalized gradient approximation (GGA) for $\mathcal{T}_s$ and its associated entropy functional, thus providing a nonempirical noninteracting free energy functional $\mathcal{F}_s$. It extends and rationalizes the recently published constraint-based, but empirically parametrized GGA.[11] We show that this nonempirical functional makes OFDFT-AIMD competitive with finite-T KS-AIMD calculations for accuracy and much faster. For deuterium in the WDM regime, the OFDFT AIMD and reference KS results agree well at intermediate T, $6\times10^4 \rightarrow 1.8\times10^5$ K. In the range $2\times10^5 \rightarrow 4\times10^6$ K, where computational cost makes KS-AIMD data unavailable, the OFDFT AIMD and all-electron PIMC results[12] compare well. Similarly, the OFDFT-AIMD electron heat capacities for H at different material densities agree well with reference KS calculations up to $T = 1\times10^6$ K.

Reference 11 showed that well-behaved noninteracting free-energy GGA functionals should be defined in terms of distinct KE and entropic enhancement factors, $F_\tau(s_\tau)$ and $F_\sigma(s_\sigma)$, and showed that a useful approximation to their exact thermodynamic relationship is $F_\sigma(s_\sigma) \approx 2 - F_\tau(s_\sigma)$. Each is a function of reduced density gradients with distinct explicit T dependence, $s_\tau(n,\nabla n,t)$ and $s_\sigma(n,\nabla n,t)$, shown in detail in Ref. 11. Here the reduced temperature is $t = T/T_\mathrm{F} = 2/\beta[3\pi^2 n(\mathbf{r})]^{2/3}$, with $\beta = (k_\mathrm{B}T)^{-1}$. Both s_τ and s_σ go to the reduced density gradient familiar in exchange GGA functionals, $s(n,\nabla n) = |\nabla n|/\{2(3\pi^2)^{1/3}n^{4/3}\}$ as $T \rightarrow 0$ K. The GGA form for the noninteracting (KS system) free energy thus is

$$\mathcal{F}_\mathrm{s}^\mathrm{GGA}[n,T] = \int d\mathbf{r}\tau_0^\mathrm{TF}(n)\{\xi(t)F_\tau(s_\tau) - \zeta(t)F_\sigma(s_\sigma)\}, \qquad (1)$$

where τ_0^TF is the zero-T TF KE density. The functions $\xi(t)$ and $\zeta(t)$ are smooth, well-behaved combinations of Fermi-Dirac integrals, with forms given explicitly in Ref. 11. The unaddressed problem in Ref. 11, which we resolve here, is how to get a reliable, wholly nonempirical representation of F_τ.

In Eq. (1), t appears such that the $T = 0$ K limit of the GGA free energy is a ground-state OF-KE functional defined by the enhancement factor $F_\tau(s)$; that is,

$$\lim_{T\rightarrow0}\mathcal{F}_\mathrm{s}^\mathrm{GGA}[n,T] = \int d\mathbf{r}\tau_0^\mathrm{TF}(n)F_\tau(s) = \mathrm{T}_\mathrm{s}^\mathrm{GGA}[n]. \qquad (2)$$

Therefore the enhancement factor $F_\tau(s)$ and the functional Eq. (2) are subject to $T = 0$ K KE constraints. These include (i) recovery of the second-order gradient expansion (GE) in the small-s limit,[13] $F_\tau(s) \approx 1 + (5/27)s^2$; (ii) a nonnegative Pauli potential,[14–16]

$$v_\theta([n];\mathbf{r}) := \frac{\delta\mathrm{T}_\theta}{\delta n} \equiv \frac{\delta(\mathrm{T}_\mathrm{s}[n] - \mathrm{T}_\mathrm{vW}[n])}{\delta n(\mathbf{r})} \geqslant 0,\ \forall\ \mathbf{r}, \qquad (3)$$

with $\mathrm{T}_\mathrm{vW}[n] = \int d\mathbf{r}\tau_0^\mathrm{TF}(n)(5s^2/3)$ the von Weizsäcker (vW) functional;[17] and (iii) recovery of vW behavior in the large-s limit.

Constraint (i) guarantees a correct description for uniform and slow-varying densities. As shown in Refs. 18,19, positivity of v_θ is required to achieve molecular and solid binding. Constraint (iii) follows from the character of charge densities

far from any nucleus and the so-called IP theorem.[15] However, the analytical form of the KE enhancement factor is a matter of design choice, sometimes motivated by the conjointness conjecture,[20] to wit $F_\tau(s) \propto F_x(s)$. Thus, the nonempirical APBEK[21] $T = 0$ K functional uses the PBE X enhancement factor form.[22] Manifestly it violates constraint (iii). As to (i), the GE coefficient for APBEK is 0.23889, which corresponds to the modified gradient expansion.[21] But v_θ from APBEK violates constraint (ii) in that $v_\theta^{\mathrm{APBEK}}$ has negative singularities at nuclear positions. The behavior of v_θ near a nucleus, $r \approx 0$ follows from the Kato nuclear-cusp condition[23]

$$n(r) \sim e^{-2Zr} = (1 - 2Zr) + O(r^2). \tag{4}$$

Thus $v_\theta^{\mathrm{APBEK}}(r) \sim a/r$ with $a < 0$ for $r \approx 0$.

To satisfy constraints (i) and (ii) simultaneously and incorporate (iii) therefore requires a more flexible form. Constraint (iii) also occurs in the VT{84} X enhancement factor,[24] so we adopt a suitably modified form for F_τ,

$$F_\tau^{\mathrm{VT84F}}(s) = 1 - \frac{\mu s^2 e^{-\alpha s^2}}{1 + \mu s^2} + (1 - e^{-\alpha s^m})(s^{-n} - 1) + \frac{5s^2}{3}, \tag{5}$$

with $m = 8$, $n = 4$. ("F" in "VT84F" denotes this free-energy adaptation.) The last term in Eq. (5) provides the correct large-s limit, constraint (iii). The parameters μ and α then must be determined from constraints (i) and (ii). Expansion of Eq. (5) at small s gives $F_\tau^{\mathrm{VT84F}}(s) = 1 + (5/3 + \alpha - \mu)s^2 + O(s^4)$. Constraint (i) imposes a relation between the two parameters, $\alpha = \mu - 5/3 + 5/27$. Evaluation of the Pauli potential for small r from the density Eq. (4) shows that the singular term a/r becomes marginally positive for $\mu = 2.778$. That gives $\alpha = 1.2965$. Equation (5) then fixes the kinetic and entropic enhancement factors in the free-energy functional Eq. (1), $F_\tau^{\mathrm{VT84F}}(s_\tau)$ and $F_\sigma^{\mathrm{VT84F}}(s_\sigma) = 2 - F_\tau^{\mathrm{VT84F}}(s_\sigma)$. For comparison, we also built the noninteracting free-energy functional APBEF from the zero-T APBEK KE[21] by use of the same prescription; that is, $F_\tau^{\mathrm{APBEF}}(s_\tau) = 1 + \mu s_\tau^2/(1 + s_\tau^2\mu/\kappa)$ and $F_\sigma^{\mathrm{APBEF}}(s_\sigma) = 2 - F_\tau^{\mathrm{APBEF}}(s_\sigma)$ with $\mu = 0.23889$, $\kappa = 0.804$.

Figure 1 shows the two main differences between the VT84F and APBEF Pauli enhancement factors, $F_\tau(s) - (5s^2/3)$. For VT84F, $F_\tau(s) - (5s^2/3)$ is nonnegative and vanishes at large s and has positive slope near $s \approx 0.39$ to provide the correct sign of the corresponding $v_\theta^{\mathrm{VT84F}}$ near nuclear sites. APBEF has neither feature. At small s,

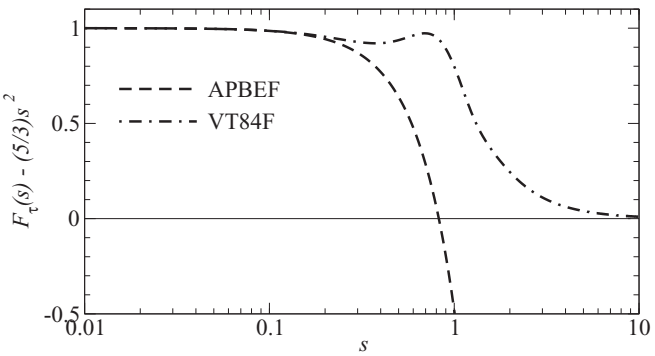

FIG. 1. VT84F and APBEF Pauli term enhancement factors $F_\tau(s) - (5s^2/3)$ as a function of s ($T = 0$ K).

TABLE I. Equilibrium lattice constants a and bulk moduli B calculated with the VT84F KE functional. OFDFT calculations with APBEK do not yield equilibrium configurations. KS LDA values are shown for comparison. All OFDFT calculations with T-independent LDA XC (Ref. 28).

System/Method	a (Å)	B (GPa)
sc-H		
OFDFT (VT84F + LDA)	1.353	175.3
KS (LDA)[11]	1.446	108.4
fcc-Al		
OFDFT (VT84F + LDA)	4.095	120.4
KS (LDA)[29]	4.020	79.66

both functions have similar behavior defined by the gradient expansion with similar coefficients.

We have implemented these functionals in a modified version of the PROFESS[25] code which we have interfaced to the QUANTUM ESPRESSO code[26] to support KS and OFDFT AIMD calculations on the same footing.[27] The data in Table I illustrate the critical importance of satisfying constraint Eq. (3). [Both these calculations used Perdew-Zunger local density approximation (LDA) exchange correlation (XC).[28]] At $T = 0$ K, the VT84F KE functional gives binding in sc-H and fcc-Al with lattice constants underestimated by about 6% for sc-H and about 2% for fcc-Al. The APBEK functional has typical ordinary GGA KE functional behavior. It fails to yield binding because of violation of constraint Eq. (3).[18] The bulk moduli from VT84F, however, are higher than the reference KS values.

To test the OF functionals at finite T, we started from static calculations with cold nuclei and hot electrons. Such a situation arises, for example, when a target is irradiated by a femtosecond laser pulse.[30] Calculations were done for sc-H at material density $\rho_{\mathrm{H}} = 0.60$ and 2.0 g/cm^3 (r_s =1.650 and 1.105 bohrs, respectively) with 64 atoms in the simulation cell. The reference KS calculations used 8 atoms in a supercell and a $13 \times 13 \times 13$ Monkhorst-Pack Brillouin zone grid.[31] Our transferable PAW data set[32] was employed in the KS calculations, and a similarly transferable local pseudopotential[11] was used in the OFDFT calculations. For this stage of testing, ordinary PZ LDA XC again was used.[28] Owing to machine-time limitations, we were able to complete KS calculations only up to $T = 4 \times 10^5$ K for $\rho_{\mathrm{H}} = 0.60$ g/cm^3 and to 10^6 K for $\rho_{\mathrm{H}} = 2.0$ g/cm^3.

Figure 2 compares the electronic heat capacity, $C_{\mathrm{V}}^{\mathrm{el}} = (\partial E^{\mathrm{el}}/\partial T_{\mathrm{el}})_{\mathrm{V}}$, where E^{el} is the electronic internal energy and T_{el} is the electronic temperature and the units are per atom. At low T, $C_{\mathrm{V}}^{\mathrm{el}}$ goes linearly with T. In the high-T limit, it goes to the classical ideal gas value, $(3/2)k_{\mathrm{B}} = 4.750$ hartrees/MK per particle. Values from our VT84F functional agree quite well with the KS data for the whole range of T, except for a small deviation near 80 kK for $\rho_{\mathrm{H}} = 0.60$ g/cm^3. Both the VT84F and KS values exhibit only a weak dependence on material density and converge slowly to the TF limit, which is reached at $T \approx 1500$ kK. By comparison, $C_{\mathrm{V}}^{\mathrm{el}}$ values from the APBEF and TF functionals agree well with the KS data for low T, up to about 60 kK for $\rho_{\mathrm{H}} = 2.0$ g/cm^3. But for the lower density, the APBEF results deviate from the KS data up to 20% for

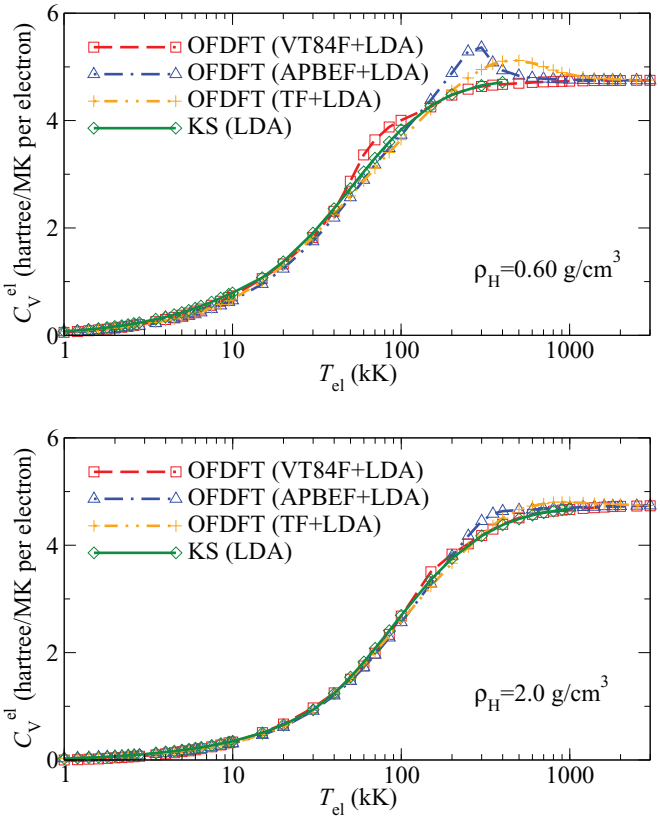

FIG. 2. (Color online) Electronic heat capacity, C_V^{el}, as a function of electronic T for sc-H at material density $\rho_H = 0.60$ and 2.0 g/cm^3.

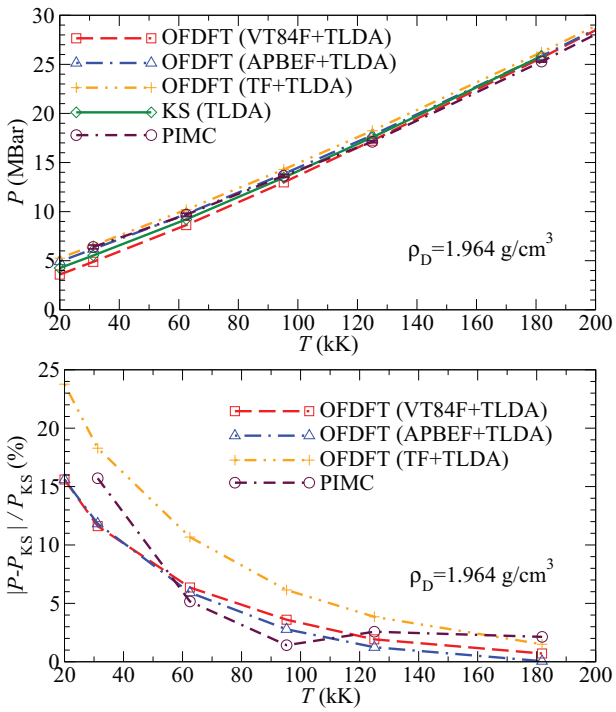

FIG. 3. (Color online) Upper panel: Pressures for OFDFT and KS AIMD, both with explicitly T-dependent XC (Ref. 34) compared with PIMC (Ref. 12) results for deuterium at $\rho_D = 1.964$ g/cm^3 ($r_s = 1.40$ bohrs). Lower panel: Relative differences of OFDFT and PIMC pressures with respect to KS values.

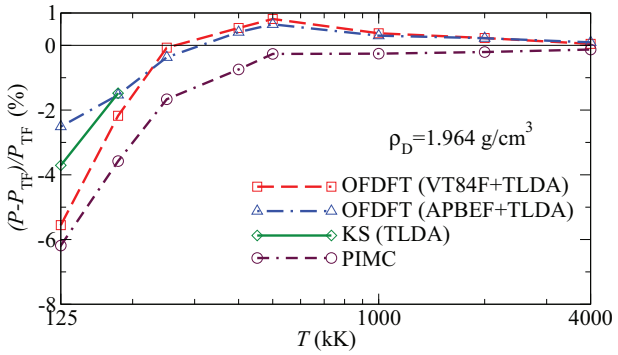

FIG. 4. (Color online) Excess pressure relative to the TF model for OFDFT (APBEK and VT84F functionals), KS and PIMC (Ref. 12), for deuterium at material density $\rho_D = 1.964$ g/cm^3 ($r_s = 1.40$ bohrs).

T_{el} between approximately 150 kK and 600 kK, whereas the TF results have a comparable deviation in the range of about 200 kK $\leqslant T \leqslant$ 900 kK. A technical point is that the second derivative discontinuity of fits used in the OFDFT calculations (see Ref. 11) affects the OFDFT results for C_V^{el} at $T \approx T_F/2$.

The second finite-T test of our functional was to calculate the deuterium equation of state (EOS) in the WDM regime.[33] All the AIMD simulations were performed with 64–512 atoms in the simulation cell (depending on material density) using the NVT ensemble regulated by the Andersen thermostat. For KS calculations at $T \leqslant 31\,250$ K, we used a $3 \times 3 \times 3$ Monkhorst-Pack k grid,[31] while for higher T a single Γ point was used. All the calculations used an explicitly T-dependent LDA (TLDA) XC functional;[34] see Ref. 32 for justification.

The upper panel of Fig. 3 compares pressures for deuterium at $\rho_D = 1.964$ g/cm^3 ($r_s = 1.40$ bohrs) from OFDFT and KS AIMD simulations, along with PIMC results. Our VT84F functional tends to underestimate the pressure while both TF and APBEF overestimate it. However, our functional reduces the error at $T = 200$ kK to 15% compared to the TF error of 24%. Note that APBEF, which fails to predict an equilibrium ground state, nevertheless gives about the same relative pressure error as VT84F, hence provides an inconsistent description. The error in the OFDFT values decreases with increasing T, such that at $T = 95\,250$ K that error is about 3% for the two GGAs versus 6% for TF. At $T = 181\,825$ K (the

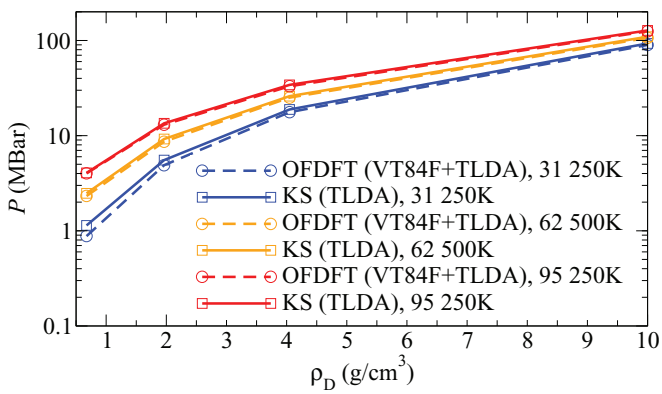

FIG. 5. (Color online) Pressure vs material density for selected temperatures calculated by OFDFT and KS AIMD for deuterium.

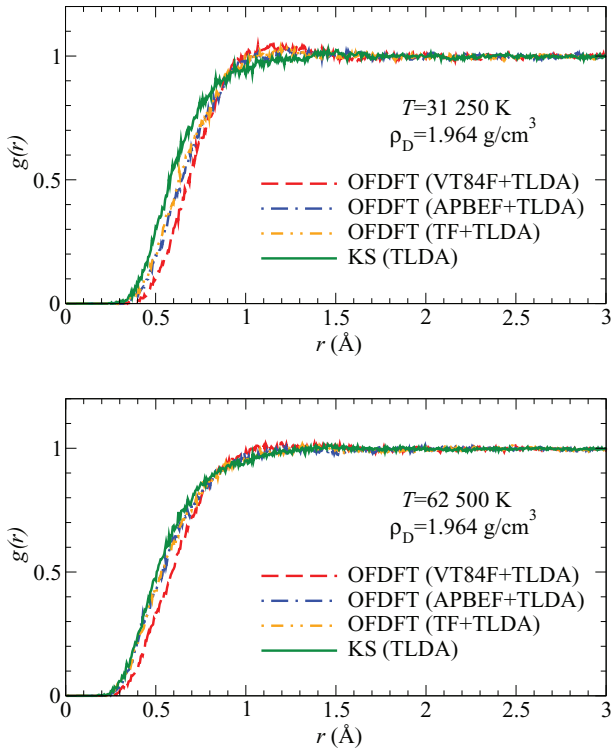

FIG. 6. (Color online) The OFDFT and KS ion pair-correlation function for $T = 31\,250$ K (upper panel) and $T = 62\,500$ K (lower panel).

highest T for which we were able to complete the KS AIMD simulation), that error is 1.5% for TF compared to tenths of a percent for VT84F (and for APBEF as well). Comparison of PIMC to KS gives relative differences of essentially the same magnitude as the OFDFT calculations which use our functionals. At the lowest temperature, $T = 31\,250$ K, PIMC overestimates the pressure by 15%, with the error decreasing rapidly with increasing T.

In the high-T TF limit, the system goes over to a fully ionized electron-ion plasma. Figure 4 shows the excess pressure relative to the TF model for $125\,000 \leqslant T \leqslant 4\,000\,000$ K. For $T = 125\,000$ and 181 825 K, where KS data are available, both VT84F and APBEF provide excellent agreement (within about 2%). Our OFDFT results also are in reasonably good agreement with the PIMC data (almost within the margin of numerical error).

Figure 5 compares KS and OFDFT pressures for deuterium as a function of ρ_D for three temperatures. The small deviations of the values from the VT84F functional with respect to the KS values at lowest density, $\rho_D = 0.674$ g/cm^3, $T = 31\,250$ K, diminish quickly with increasing ρ_D or increasing T.

Figure 6 compares KS and OFDFT ion pair-correlation functions (PCF) for two temperatures. The upper panel ($T = 31\,250$ K) demonstrates that all the OFDFT calculations

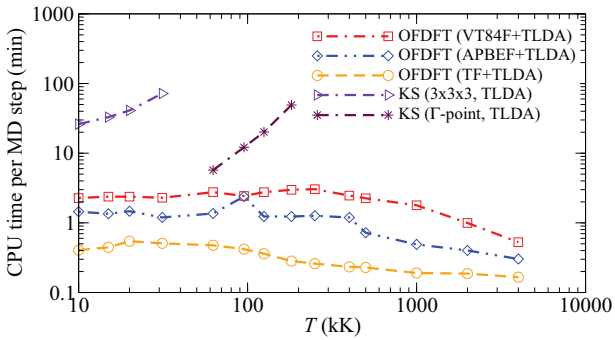

FIG. 7. (Color online) CPU time per AIMD step as a function of T for OFDFT-MD calculations compared to the KS-MD data. Deuterium at $\rho_D = 1.964$ g/cm^3 ($r_s = 1.40$ bohrs), 128 atoms in simulation cell.

predict structural properties at this temperature in reasonable agreement with the KS results, except for some discrepancies (peaks) near $r = 1.0$ Å. We suspect, but have not been able to confirm, that those peaks are related to nuclear site singularities in the GGA Pauli potential, Eq. (3). Those singularities could lead to peaks such as seen in hard- or soft-sphere liquid PCFs.[35] Note also that the peaks are consistent with the overly large bulk moduli via the compressibility sum rule; see Eq. (3.16) in Ref. 36. In any event, for $T = 62\,500$ K and above, the agreement between OFDFT and KS PCFs becomes satisfactory.

Comparison of computational times per AIMD step for OFDFT and KS is in Fig. 7. The calculations were done on a single CPU to provide the most favorable case for KS (no parallel overhead). The OFDFT timings are essentially independent of T and faster than corresponding KS AIMD runs by from one to two orders of magnitude for the range of T shown. In practice, the KS calculations typically need 8 to 64 CPUs for reasonable turnaround. In that case, the OFDFT advantage is substantially greater.

In summary, we have presented a wholly nonempirical parametrization of a ground-state orbital-free KE functional and used it to generate kinetic and entropic noninteracting free-energy functionals. These functionals have several virtues. First, the ground-state part gives a reasonable description of the ground-state solid for sc-H and fcc Al, something not achieved by any other nonempirical KE GGA. Second, the consequent free-energy functionals give good WDM properties for sc-H in the static lattice case (e.g., electronic heat capacity) and provide a competitive-quality AIMD simulation of the deuterium EOS. All of this is with the long-promised computational speed advantage of OFDFT.

We thank T. Sjostrom for valuable discussions. This work was supported by the U.S. Department of Energy TMS Grant No. DE-SC0002139. We also acknowledge the University of Florida High-Performance Computing Center for providing computational resources and technical assistance.

*vkarasev@qtp.ufl.edu

[1] M. P. Surh, T. W. Barbee III, and L. H. Yang, Phys. Rev. Lett. **86**, 5958 (2001).

[2] K. P. Driver and B. Militzer, Phys. Rev. Lett. **108**, 115502 (2012).

[3] *Basic Research Needs for High Energy Density Laboratory Physics* (Report of the Workshop on Research Needs, Nov. 2009). U.S. Department of Energy, Office of Science and National Nuclear Security Administration (2010); see Chap. 6 and references therein.

[4]M. P. Desjarlais, J. D. Kress, and L. A. Collins, Phys. Rev. E **66**, 025401 (2002).
[5]D. A. Horner, F. Lambert, J. D. Kress, and L. A. Collins, Phys. Rev. B **80**, 024305 (2009).
[6]N. D. Mermin, Phys. Rev. **137**, A1441 (1965).
[7]M. V. Stoitsov and I. Zh. Petkov, Ann. Phys. **185**, 121 (1988).
[8]R. M. Dreizler, in *The Nuclear Equation of State*, Part A, edited by W. Greiner and H. Stöcker, NATO ASI Ser. B Vol. 216 (Plenum, New York, 1989), p. 521.
[9]R. P. Feynman, N. Metropolis, and E. Teller, Phys. Rev. **75**, 1561 (1949).
[10]J. Xia and E. A. Carter, Phys. Rev. B **86**, 235109 (2012), and references therein.
[11]V. V. Karasiev, T. Sjostrom, and S. B. Trickey, Phys. Rev. B **86**, 115101 (2012).
[12]S. X. Hu, B. Militzer, V. N. Goncharov, and S. Skupsky, Phys. Rev. B **84**, 224109 (2011).
[13]C. H. Hodges, Can. J. Phys. **51**, 1428 (1973).
[14]M. Levy and Hui Ou-Yang, Phys. Rev. A **38**, 625 (1988).
[15]M. Levy, J. P. Perdew, and V. Sahni, Phys. Rev. A **30**, 2745 (1984).
[16]C. Herring, Phys. Rev. A **34**, 2614 (1986).
[17]C. F. von Weizsäcker, Z. Phys. **96**, 431 (1935).
[18]V. V. Karasiev, R. S. Jones, S. B. Trickey, and F. E. Harris, Phys. Rev. B **80**, 245120 (2009).
[19]V. V. Karasiev and S. B. Trickey, Comput. Phys. Commun. **183**, 2519 (2012).
[20]H. Lee, C. Lee, and R. G. Parr, Phys. Rev. A **44**, 768 (1991).
[21]L. A. Constantin, E. Fabiano, S. Laricchia, and F. Della Sala, Phys. Rev. Lett. **106**, 186406 (2011).
[22]J. P. Perdew, K. Burke, and M. Ernzerhof, Phys. Rev. Lett. **77**, 3865 (1996); **78**, 1396(E) (1997).
[23]T. Kato, Commun. Pure Appl. Math. **10**, 151 (1957).
[24]A. Vela, J. C. Pacheco-Kato, J. L. Gázquez, J. M. del Campo, and S. B. Trickey, J. Chem. Phys. **136**, 144115 (2012).
[25]G. S. Ho, V. L. Lignères, and E. A. Carter, Comput. Phys. Commun. **179**, 839 (2008); L. Hung, C. Huang, I. Shin, G. S. Ho, V. L. Lignères, and E. A. Carter, *ibid*. **181**, 2208 (2010).
[26]P. Giannozzi *et al*., J. Phys.: Condens. Matter **21**, 395502 (2009).
[27]V. V. Karasiev, T. Sjostrom, and S. B. Trickey (unpublished).
[28]J. P. Perdew and A. Zunger, Phys. Rev. B **23**, 5048 (1981).
[29]J. C. Boettger and S. B. Trickey, Phys. Rev. B **53**, 3007 (1996).
[30]R. Ernstorfer, M. Harb, C. T. Hebeisen, G. Sciaini, T. Dartigalongue, and R. J. D. Miller, Science **323**, 1033 (2009).
[31]H. J. Monkhorst and J. D. Pack, Phys. Rev. B **13**, 5188 (1976).
[32]V. V. Karasiev, T. Sjostrom, and S. B. Trickey, Phys. Rev. E **86**, 056704 (2012).
[33]J. M. McMahon, M. A. Morales, C. Pierleoni, and D. M. Ceperley, Rev. Mod. Phys. **84**, 1607 (2012).
[34]F. Perrot and M. W. C. Dharma-wardana, Phys. Rev. B **62**, 16536 (2000); **67**, 079901 (2003).
[35]H. C. Anderson, J. D. Weeks, and D. Chandler, Phys. Rev. A **4**, 1597 (1971).
[36]J. S. Rowlinson, Rep. Prog. Phys. **28**, 169 (1965).